

Rims of carbon nanotubes – influence of chirality

Heiko Dumlich* and Stephanie Reich

Fachbereich Physik, Freie Universität Berlin, Arnimallee 14, 14195 Berlin, Germany

Received 4 May 2010, revised 28 July 2010, accepted 5 August 2010

Published online 13 September 2010

Keywords carbon nanotube, chirality, nanotube composites, NEMS, Rim, structure

*Corresponding author: e-mail heiko.dumlich@fu-berlin.de, Phone: +49 30 83856157, Fax: +49 30 83856081

We study the possible configurations of the open ends (rims) of carbon nanotubes. There are many possible rim structures for a given chirality (n,m) . The rim configuration depends to a large extent on the atomic species and shape of its host material. We develop formulas to derive the number of armchair and zigzag-type dangling bonds contained in a specific rim configuration.

Armchair and zigzag-type dangling bonds form different barriers at the interface between a carbon nanotube and a host material. Reshaping the rim to a desired configuration allows to change the properties of the nanotube, e.g. transport barriers, which might be interesting for producing tailored NEMS or carbon nanotube based composites.

© 2010 WILEY-VCH Verlag GmbH & Co. KGaA, Weinheim

1 Introduction Carbon nanotubes are a fascinating material with largely varying electrical and mechanical properties depending on the atom configuration/chirality [1]. Many studies have been devoted to determine how nanotube properties depend upon chirality, e.g. electronic structure [2, 3]. The possible nanotube cap configurations have been extensively studied [4, 5], which fix the chirality of the nanotube [6]. But so far no extensive study of the rims of carbon nanotubes in chirality dependence has been conducted.

Most studies considering the rim only treated the rim structure as a byproduct of growth [7–10]. The growth is modelled with addition of carbon atoms or carbon dimers. Gomez-Gualdrón and Balbuena [8] start with preformed caps in inclined rim configurations and add C_2 until straight rim configurations are achieved. The addition paths allow to derive various rim configurations, but as the aim of the study was to understand the growth, no detailed study on the rim configurations was performed. Ding et al. [9] showed that achiral tubes (armchair and zigzag nanotubes) will only grow with the introduction of kinks.

In this paper we study various rim configurations in dependence of nanotube chirality. We demonstrate how to derive all possible rim configurations. We find that rim configurations can be described by formulas depending on the chiral indexes (n,m) and the number of kinks, which correspond to addition of C_2 between two armchair sites. Designing the environment of carbon nanotube rims to certain shapes, by, e.g. lithographic methods, allows to

obtain specific rim configurations with properties that can be interesting for the implementation into NEMS. Understanding the rim shaping is further important to understand and design carbon nanotube based composites, as the interfaces between the nanotubes and the composite material influence the properties of the whole system. Manipulating the rim structure of a nanotube opens a new field for tailoring the properties of carbon nanotubes and nanotube devices.

2 Rims of carbon nanotubes We first want to derive possible rims of a carbon nanotube. Therefore we first define the elements which a nanotube rim can be composed of, using an example including all the elements. A three-dimensional wire model of a $(5,5)$ nanotube with two different rim structures and an unzipped two-dimensional representation of the rims are shown in Fig. 1. In general there are two kinds of dangling bonds – armchair a and zigzag z – that exist in a nanotube rim. Armchair dangling bonds a consist of one of two neighbouring twofold C–C bonded atoms. Zigzag dangling bonds z have two saturated C neighbours and are themselves twofold C–C bonded. An addition site denoted by ‘.’ elongates the rim by a hexagon with C_2 addition. The rim presented in Fig. 1a is the one expected from the circumferential chiral vector construction. The rim of Fig. 1b is another possible rim with one side being much longer than the other side, this produces an angled end of the tube.

© 2010 WILEY-VCH Verlag GmbH & Co. KGaA, Weinheim

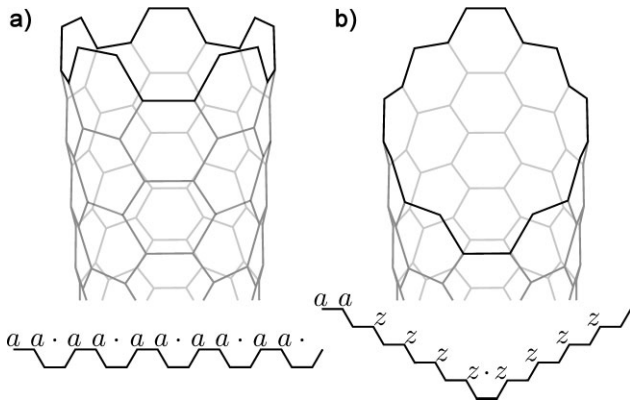


Figure 1 3d wire model of a (5,5) nanotube and unzipped 2d representation of its rim. Addition sites ‘.’ armchair ‘a’ and zigzag dangling bonds ‘z’ are the elements that a rim contains. (a) From circumferential vector expected rim and (b) Angled rim.

To derive all possible nanotube rims containing only armchair and zigzag dangling bonds, we use the rim creation sheet presented in Fig. 2. The possible rim paths for a (3,3) nanotube [11] are shown bordered by full lines. Following the direct connection between the lower corner of the (0,0) hexagon to the (3,3) hexagon yields the rim we expect from the chiral vector, see Fig. 3 (0.0₃). The number of armchair $N_a = 2 \cdot m$ and zigzag dangling bonds $N_z = n - m$ for this rim configuration depend solely on the chirality. Following the rim in Fig. 1a from left to right leads to the notation of the particular rim configuration: *aa.aa.aa.aa.aa.*, which has $N_a = 10$ and $N_z = 0$. An angled rim has $N_a = 2$ and $N_z = n + m - 2$, with $m \neq 0$, and it can be obtained by following the other full line path between (0,0) and (3,3). It has a *aa(n-1)z.(m-1)z* rim structure. All the paths inside of the borders created by the full lines in Fig. 2 lead to different rim configurations, which have to fulfill the condition $N_a + N_z = n + m$. There are simple rules to derive a rim from the rim creation sheet: (i) The route must not go in

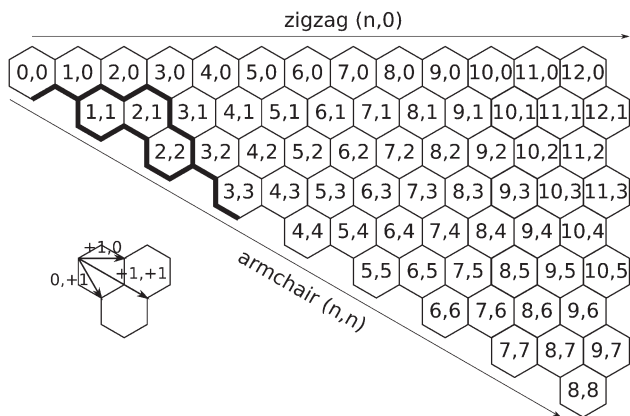


Figure 2 Rim creation sheet with the possible rim paths for a (3,3) nanotube. Connecting the lower corner of the (0,0) hexagon with the lower corner of the (3,3) hexagon by any of the paths inside of the full line border yields a (3,3) rim.

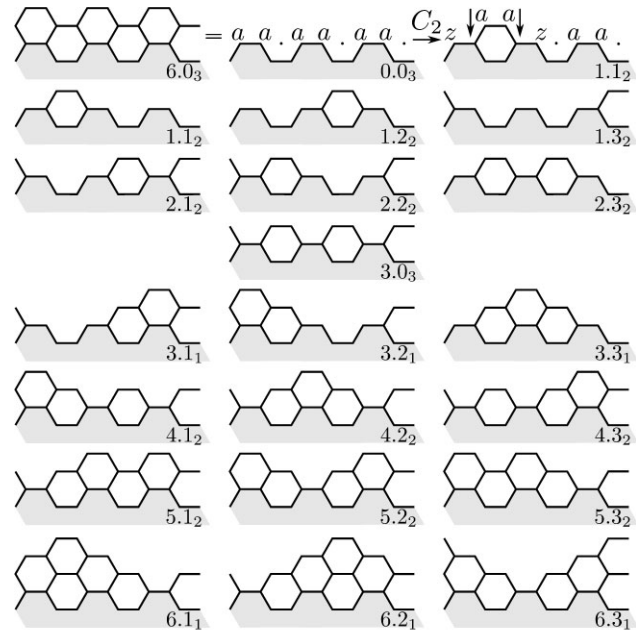


Figure 3 All possible (3,3)-armchair nanotube rims from C_2 addition. The numbers at the bottom right of the rims are defined by $A.B_C$ with A the number of added C_2 , B a counting variable for different rims (0 is special, as these are half or full layers) and C the number of addition sites. The grey shaded side represents the body of the tube.

circles, (ii) borders are not allowed to be crossed and (iii) paths only include \uparrow up, \swarrow down-left and \nwarrow up-left steps.

The rim configurations derived by the rim creation sheet are presented in Fig. 3. The numbers at the bottom right of the rims are defined by $A.B_C$ where A denotes the number of added C_2 compared to the rim derived from the circumferential vector, B is a counting variable for different rims (0 is special, as these are half or full layers) and C is the number of addition sites.

The amount of carbon atoms that needs to be added to complete a full layer depends on the chirality and is equal to the number of rim atoms $2 \cdot (n + m)$. For a (3,3) tube the addition of $n + m = 6$ C_2 to a rim structure can lead to a symmetrically equivalent rim structure, e.g. $0.0_3 = 6.0_3$ or $1.3_2 = 7.3_2$.

In the first line of Fig. 3 ($0.0_3 \rightarrow 1.1_2$) we introduce the armchair kinks; A kink occurs in Fig. 3 (1.1₂) at the first \downarrow as in the rim expected for the chiral vector the path would have to go down. At the second \downarrow in Fig. 3 (1.1₂) another kink occurs and the remaining rim corresponds to the rim structure expected from the chiral vector. Two armchair kinks are equal to a C_2 addition between two armchair sites of the rim, changing the rim configuration by transformation of $2a$ into $2z$ dangling bonds. With the number of armchair kinks $k = 2 \cdot x$, ($x = 0, 1, \dots, m-2, m-1$), we can derive all m possible rim configurations in dependence of N_a and N_z

$$N_a = 2 \cdot m - k, \tag{1}$$

$$N_z = n - m + k. \quad (2)$$

The maximal number of armchair kinks in a rim is $k_{\max} = 2 \cdot (m - 1)$. From Fig. 3 it is clear that the number of possible rims for a certain chirality is not equal to the number of possible rim configurations depending on N_a and N_z . Various configurations, however 1.1₂, 1.2₂ and 1.3₂ are identical by symmetry, allowing for a reduction to the m rim configurations designated by N_a and N_z .

Up to now we only treated a rim of an achiral (armchair) tube. But similar considerations are applicable to chiral tubes. In Fig. 4 we present rims of a (6,4) tube, constructed with the rim creation sheet. The addition to different addition sites at the rim yields different transitions for the rim configuration. We can derive three kinds of growth sites $aa.aa$, $aa.z$ and $z.z$, with $z.aa$ being equal to $aa.z$ by symmetry. Addition to other rim sites, aa , az , za and zz does not add hexagons and is therefore suppressed by energetical reasons. Table 1 presents all rim sites and the transitions for growth sites. Addition of C_2 to an $aa.aa$ growth site induces a transition $aa.aa \rightarrow zaa.z$ removing a growth site. For $aa.z$ we have a $aa.z \rightarrow zaa.$ transition with C_2 addition, which shifts the dangling bonds and the growth sites. The C_2 addition to $z.z$ induces a transition $z.z \rightarrow .aa.$ adding a growth site to the rim. It is possible to create a different growth site type with C_2 addition to a growth site, as dangling bonds and growth sites are moved and transformed.

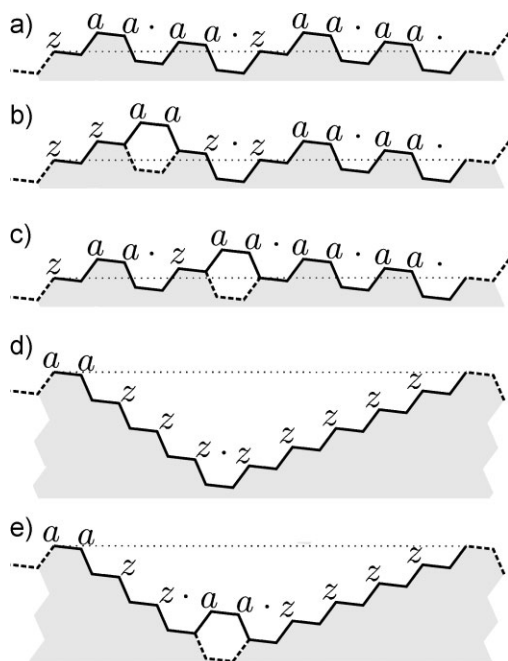


Figure 4 Various rims of a (6,4) nanotube with different rim sites. (a) Expected rim configuration. (b) After C_2 addition to (a) at $aa.aa$, removing an addition site. (c) After C_2 addition to (a) at $aa.z$, moving the addition site. (d) Most angled rim of the (6,4) tube. (e) After C_2 addition to (d) at $z.z$, adding an addition site.

Table 1 Overview of site types in a nanotube rim. ‘ Δ .’ represents the change in addition site number and ‘transition’ the change of the bond structure with C_2 addition.

site	Δ .	transition	example
$aa.aa$	-1	$aa.aa \rightarrow zaa.z$	Fig. 4a→b
$aa.z/z.aa$	0	$aa.z \rightarrow zaa./z.aa \rightarrow .aa.z$	Fig. 4a→c
$z.z$	+1	$z.z \rightarrow .aa.$	Fig. 4d→e
aa	-	-	Fig. 4e
az/za	-	-	Fig. 4b
zz	-	-	Fig. 4d

The rims of carbon nanotubes contain different numbers of growth sites depending on chiral indexes (n, m) and the exact rim configuration. The number of growth sites in the rim configuration derived from the circumferential vector (e.g. 6.0₃ configuration in Fig. 3 and Fig. 4a) are

$$N_{aa.aa} = \begin{cases} 2m-n & \text{if } 2m-n > 0 \\ 0 & \text{otherwise} \end{cases}, \quad (3)$$

$$N_{aa.z} = \min(m, n-m), \quad (4)$$

and $N_{z.z} = 0$. All chiral tubes have at least one $aa.z$ site in the rim configuration derived from the circumferential vector at which growth can occur without inducing armchair kinks. The chiral selectivity of the growth process of carbon nanotubes can be derived from the chirality dependent number and type of growth sites in the rim, which also changes during the elongation of the nanotube [13].

The rim configuration depends on the environment of the rim. The rim is deformed if its environment is taken into account. In vacuum the dangling bonds tend to bend out of the nanotube axis and the rim atoms decrease their nearest neighbour distances [14, 15]. Rims in contact with other atomic species, e.g. a metallic catalyst, interact with the surface of the catalyst and the rims are deformed according to the surface structure [6]. Therefore the rim expected from the circumferential vector is not in every case the most likely rim, as a preformed contact can force the nanotube rim into a certain rim configuration. This is an important aspect which can be used to create tailored NEMS. Angled rims are expected to show different transport barriers compared to rims expected from the chiral vector as the dangling bond structure is changed. This allows to tailor the host material to fit a certain rim structure, which manipulates the barriers that develop between the nanotube and host material interface. Further if carbon nanotube based composites are considered, it is possible to manipulate, e.g. the elastic or thermal properties by the interface shape.

3 Conclusion In summary, we presented and studied various rim configurations of carbon nanotubes. We showed how to derive the rim configurations with the help of simple geometrical methods. Rims consist of armchair

dangling bonds, zigzag dangling bonds and addition sites, which together constitute three different kinds of growth sites. Rims depend on chirality and the exact rim configuration which influence the angle of the tube end. The rims of carbon nanotubes with equal chirality have a varying distribution of zigzag and armchair dangling bonds depending on the rim configuration. Carbon nanotubes of the same chirality can contain, e.g. different energy barriers for electronic transport. The environment of the nanotube shapes the rim and therefore opens a new field of designing tailored NEMS contacts and nanotube based composites.

Acknowledgements We acknowledge useful discussions with J. Robertson and S. Heeg. This work was supported by ERC grant no. 210642.

References

- [1] S. Reich, C. Thomsen, and J. Maultzsch, *Carbon Nanotubes* (Wiley VCH, Berlin, 2003), Chap. 2.
- [2] N. Hamada, S. Sawada, and A. Oshiyama, *Phys. Rev. Lett.* **68**, 1579–1581 (1992).
- [3] R. Saito, M. Fujita, G. Dresselhaus, and M. S. Dresselhaus, *Phys. Rev. B* **46**, 1804–1811 (1992).
- [4] G. Brinkmann, P. W. Fowler, D. E. Manolopoulos, and A. H. R. Palser, *Chem. Phys. Lett.* **315**, 335–347 (1999).
- [5] S. Reich, L. Li, and J. Robertson, *Phys. Rev. B* **72**, 165423 (2005).
- [6] S. Reich, L. Li, and J. Robertson, *Chem. Phys. Lett.* **421**, 469–472 (2006).
- [7] Y. H. Lee, S. G. Kim, and D. Tomanek, *Phys. Rev. Lett.* **78**, 2393–2396 (1997).
- [8] D. A. Gomez-Gualdrón and P. B. Balbuena, *Nanotechnology* **19**, 485604 (2008).
- [9] F. Ding, A. R. Harutyunyan, and B. I. Yakobson, *Proc. Natl. Acad. Sci. USA* **106**, 2506–2509 (2009).
- [10] Q. Wang, M. Ng, S. Yang, Y. Yang, and Y. Chen, *ACS Nano* **4**, 939–946 (2010).
- [11] The full rim path analysis for a chiral (4,2) nanotube can be found in Ref. [12].
- [12] H. Dumlich, *Growth of Carbon Nanotubes on Catalytic Metal Particles*, Diploma Thesis (FU Berlin, 2009).
- [13] H. Dumlich and S. Reich, *Phys. Rev. B* **82**, 085421 (2010).
- [14] M. Z. Hossain, *Appl. Phys. Lett.* **95**, 153104 (2009).
- [15] N. Kitamura and A. Oshiyama, *J. Phys. Soc. Jpn.* **70**, 1995–2011 (2001).